Parthenolide inhibits the tumor characteristics of renal cell carcinoma

DANDAN LIU[1*], YANYAN HAN[1,2*], LEI LIU[1], XINXIU REN[3], HAN ZHANG[1], SHUJUN FAN[1], TAO QIN[1] and LIANHONG LI[1]

[1]Department of Pathology, Dalian Medical University, Dalian, Liaoning 116044, P.R. China; [2]Department of Pathology, Okayama University Graduate School of Medicine, Dentistry, and Pharmaceutical Sciences, Okayama 700-8558, Japan; [3]Department of Biotechnology, Dalian Medical University, Dalian, Liaoning 116044, P.R. China

Received May 9, 2020; Accepted September 24, 2020

DOI: 10.3892/ijo.2020.5148

Abstract. Parthenolide has been demonstrated to have anti-cancer effects against various types of cancer. However, the functional role of parthenolid has yet to be clearly reported in renal cell carcinoma (RCC). The aim of the present study was to investigate the effect of parthenolide in RCC 786-O and ACHN cells. CCK-8 and colony-formation assays were used to observe the proliferation of RCC 786-O and ACHN cells. Migration and invasion abilities were assessed through Transwell assays. The stem cell-like properties of RCC cell lines were evaluated by mammosphere formation assay. Western blot analysis was used to investigate the metastasis and epithelial-mesenchymal transition (EMT) induced by parthenolide on the expression levels of MMP2, MMP9, E-cadherin, N-cadherin, vimentin and snail. The results revealed that when the cells were treated with various concentrations of parthenolide, the rate of proliferation and growth was decreased in 786-O and ACHN cells. The number of invasive cells in a field was approximately 170, 90, 40 and 190, 150, 70 in 786-O and ACHN cells with 0, 4 and 8 μM of parthenolide treatment. MMP-2/-9 expression ($P<0.05$) was inhibited by parthenolide. The protein levels of E-cadherin were increased ($P<0.05$) and N-cadherin, vimentin and snail were decreased ($P<0.05$) by parthenolide treatment. In addition, Parthenolide inhibited the expression of cancer stem cell markers and the PI3K/AKT pathway. The present study confirmed that parthenolide inhibited RCC cell proliferation and metastasis and suppressed the stem cell-like properties of RCC cell lines, which could be a potential strategy to treat RCC. However, further molecular mechanisms of parthenolide in RCC should be observed and reported in the future.

Correspondence to: Dr Lianhong Li, Department of Pathology, Dalian Medical University, 9 Lvshun South Road, Dalian, Liaoning 116044, P.R. China
E-mail: lilianhong@dlmedu.edu.cn

*Contributed equally

Key words: parthenolide, renal cell carcinoma, epithelial-mesenchymal transition

Introduction

Renal cell carcinoma (RCC) is one of the 14 most frequently diagnosed types of cancer worldwide and accounts for approximately 3% of all adult malignancies (1). According to the World Health Organization, the incidence and mortality rates of renal cell carcinoma (RCC) are rapidly increasing worldwide (2). Patients with RCC exhibit a trend for metastasis, and approximately 20% of them will develop metastasis following treatment (3). Surgical resection has been the major strategy in the treatment of RCC; however, this method has several limitations regarding its efficacy (4). Additionally, recent pharmacological research has indicated that targeted therapy results in the improved survival of patients with RCC (5). However, a number of patients present with metastasis following treatment, which is a main reason for the progression of RCC. Therefore, the development of novel therapeutic strategies is crucial.

The primary bioactive component of feverfew, a flowering plant in the daisy family, plant *Tanacetum parthenium*, has traditionally been used as a medicinal herb. Parthenolide has been revealed to exhibit anti-inflammatory properties, and it has been used for the treatment of migraines (6). Numerous studies have indicated that parthenolide also exhibits antitumor activity against a wide variety of solid tumors, including those of osteosarcoma, pancreatic cancer and prostate cancer (7-9). However, relevant studies have not been reported for the effects of parthenolide on EMT in RCC and renal cancer stem cells. Epithelial-mesenchymal transition (EMT) is characterized by epithelial cells under the influence of certain factors, and by a loss of cell polarity, cell connections and tight junctions, with cells acquiring a mesenchymal cell morphology and characteristics. EMT plays an important role in the regulation of tumorigenesis (10). Furthermore, the main hallmark of EMT is the loss of the expression of the adhesion molecule, E-cadherin, and the acquisition of the expression of the mesenchymal cell marker, N-cadherin (11), as well as the increase in the expression of E-cadherin transcriptional suppressors, including Snail, Twist, and Slug (11). It has been demonstrated

that the progression of metastatic RCC is usually triggered by the activation of the embryonic development program, EMT (12). Hence, targeting an important molecule that leads to this process is key to improving the treatment efficacy for RCC. It has been suggested that renal cancer stem cells (CSCs) are primarily associated with metastasis, recurrence and a poor prognosis. These cells have the ability to resist tumor therapy (13).

Therefore, the aim of the present study was to determine whether parthenolide alleviates RCC, and to examine whether parthenolide may be an effective therapeutic drug for RCC.

Materials and methods

Cell culture. 786-O and ACHN (Dalian Medical University) cells and were maintained in minimal essential medium (MEM) supplemented with 10% fetal bovine serum (FBS) and RPMI-1640 with 10% fetal bovine serum (FBS) (all from HyClone™; Thermo Fisher Scientific, Inc.), at 37˚C in a humidified atmosphere of 95% air and 5% CO_2, respectively.

Cell viability assay. A Cell Counting Kit-8 (CCK-8) (Nanjing KeyGen Biotech. Co., Ltd.) assay was used to examine cell viability. 786-O and ACHN cells were plated at a density of $5x10^3$ cells/well in 96-well plates and treated with various concentrations (0, 1, 2, 4, 6, 8, 12, 16 and 20 μM) of parthenolide (Sigma-Aldrich; Merck KGaA) for 24 and 48 h. Parthenolide was first dissolved in DMSO and serum-free medium was then used to dilute it to various concentrations (0, 1, 2, 4, 6, 8, 12, 16 and 20 μM). Thereafter, 10 μl CCK-8 solution was added to each well, and the cells were further cultured at 37˚C for 2 h. The absorbance of each group was detected using a microplate reader at a wavelength of 452 nm.

Colony-formation assay. The colony-formation assay was performed as follows: Single-cell suspensions of 786-O and ACHN cells were seeded in 6-well culture plates (1,000 cells/well). They were subsequently treated with parthenolide at various concentrations (0, 4 and 8 μM) for 24 h. Cells were cultured for a further 7 days for colony formation. The cells were then washed with phosphate-buffered saline (PBS) and fixed with 4% paraformaldehyde for 30 min at room temperature. After washing, the cells were then stained with 1% crystal violet for 20 min at room temperature, and the number of colonies (minimum number of cells in a colony was ~50) was counted. The colonies were visualized via a light microscope (magnification, x400) and were photographed using a camera.

Reverse transcription-quantitative polymerase chain reaction (RT-qPCR). 786-O and ACHN cells were incubated with parthenolide for 24 h. After incubation, total RNA was extracted using TRIzol® (Invitrogen; Thermo Fisher Scientific, Inc.), followed by isopropanol precipitation and chloroform extraction. cDNA was synthesized using the Reverse Transcriptase system (Invitrogen; Thermo Fisher Scientific, Inc.), according to the manufacturer's protocol. RT-PCR was performed using an iCycler™ Real Time system (Bio-Rad Laboratories, Inc.) and the SYBR Premix EX Tag Master mixture kit (Takara Bio, Inc.) according to the manufacturer's protocol. The PCR reactions were carried out under the following conditions: 40 cycles of denaturation at 95˚C for 10 sec, annealing at 60˚C for 20 sec and extension at 72˚C for 20 sec.

GAPDH mRNA was used as internal control. The primers used in the present study were as follows: E-cadherin forward, 5'-GAAAACAGCAAAAGGGCTTGGA-3' and reverse, 5'-TTAGGGCTGTGTACGTGCTG-3'; Snail forward, 5'-CGAGTGGTTCTTCTGCGCTA-3' and reverse, 5'-AGGGCTGCTGGAAGGTAAAC-3'; GAPDH forward, 5'-CACCCACTCCTCCACCTTTG-3' and reverse, 5'-CCACCACCCTGTTGCTGTAG-3'. The samples were amplified in different wells and run in triplicate. The relative expression of genes was calculated by means of the $2^{-\Delta\Delta Cq}$ relative quantification method (14).

Mammosphere formation assay. Following treatment with various concentrations of parthenolide for 24 h, 786-O and ACHN cell lines were inoculated into ultra-low attachment 6-well plates (Corning, Inc.) at a density of $0.1x10^6$ cells/well, and grown in MEM and RPMI-1640 supplemented with B27 (1:50, Invitrogen; Thermo Fisher Scientific, Inc.), 20 ng/ml human recombinant EGF (Sigma-Aldrich; Merck KGaA), 20 ng/ml bEGF (Sigma-Aldrich; Merck KGaA) and 5 μg/ml insulin (Sigma-Aldrich; Merck KGaA) for 14 days. Cell colonies >60 μm in diameter were counted under an inverted microscope (magnification, x400) (Olympus Corporation).

Transwell assay. Cell invasion and migration were evaluated by Transwell assays (Corning, Inc.). An 8-μm Transwell was pre-coated with diluted Matrigel (1:10 with serum-free medium; only for the cell invasion assay) and dried for 2 h at room temperature in an incubator. 786-O and ACHN cells were pretreated parthenolide (0, 4 and 8 μM) for 24 h. Briefly, $1x10^5$ cells were seeded onto each upper chamber, while medium with 10% FBS was added into the lower chamber for chemo-attraction and allowed to invade for 24 h. The Transwell chamber was then removed, the culture solution in the Transwell chamber was discarded and the chamber was washed twice with calcium-free phosphate-buffered saline (PBS). Then, the chamber was fixed in 3% methanol solution for 30 min at room temperature and stained with 0.1% crystal violet for 20 min at room temperature. The chamber was washed several times with PBS, and the upper chamber liquid was aspirated. The non-migrated/non-invasive cells in the upper layer were gently wiped off using a cotton swab. The microporous membrane was removed carefully with small tweezers and dried with the bottom side up. Next, the membrane was transferred to a glass slide and sealed with a neutral gum. Images were observed and collected by an inverted optical microscope (magnification, x200; Keyence Corporation).

Immunofluorescence analysis. Cells were seeded in a 24-well plate ($1x10^4$ cells/well) and allowed to attach overnight at 37˚C in a humidified atmosphere of 95% air and 5% CO_2. Following treatment with parthenolide (0, 4 and 8 μM) for an additional 24 h, the cells were permeabilized with 0.1% Triton X-100 for 10 min and blocked with 5% BSA (Sigma-Aldrich; Merck KGaA) for 1 h at room temperature and then incubated with primary antibodies (E-cadherin, N-cadherin, vimentin, Snail) (Table I) overnight at 4˚C. The following day, the cells were washed and incubated with AlexaFluor 594 (1:500;

Table I. Antibodies.

Primary antibodies	Clonality	Catalogue number	Company	Species	Dilution	Diluent
MMP2	Monoclonal	66366-1-Ig	ProteinTech Group, Inc.	Mouse	1:1,000	Non-fat milk
MMP9	Monoclonal	ab76003	Abcam	Rabbit	1:500	Non-fat milk
E-cadherin	Monoclonal	60335-1-Ig	ProteinTech Group, Inc.	Mouse	1:1,000	Non-fat milk
N-cadherin	Monoclonal	13116S	Cell Signaling Technology, Inc.	Rabbit	1:1,000	Non-fat milk
Vimentin	Monoclonal	60330-1-Ig	ProteinTech Group, Inc.	Mouse	1:1,000	Non-fat milk
Snail	Monoclonal	ab216347	Abcam	Rabbit	1:500	Non-fat milk
PI3K	Monoclonal	60225-1-Ig	ProteinTech Group, Inc.	Mouse	1:1,000	Non-fat milk
p-PI3K	Monoclonal	17366S	Cell Signaling Technology, Inc.	Rabbit	1:500	Non-fat milk
AKT	Monoclonal	60203-2-Ig	ProteinTech Group, Inc.	Mouse	1:1,000	Non-fat milk
p-AKT	Monoclonal	66444-1-Ig	ProteinTech Group, Inc.	Rabbit	1:1,000	Non-fat milk
ALD1H1	Monoclonal	ab52492	Abcam	Rabbit	1:500	Non-fat milk
ALD1H1	Polyclonal	22109-1-AP	ProteinTech Group, Inc.	Rabbit	1:500	Non-fat milk
CD133	Monoclonal	66666-1-Ig	ProteinTech Group, Inc.	Mouse	1:500	Non-fat milk
Oct-4	Monoclonal	60242-1-Ig	ProteinTech Group, Inc.	Mouse	1:1,000	Non-fat milk
Sox2	Monoclonal	66411-1-Ig	ProteinTech Group, Inc.	Mouse	1:1,000	Non-fat milk
GAPDH	Polyclonal	10494-1-AP	ProteinTech Group, Inc.	Rabbit	1:500	Non-fat milk
GAPDH	Monoclonal	60004-1-Ig	ProteinTech Group, Inc.	Mouse	1:500	Non-fat milk

product code ab150108) and AlexaFluor 488 (1:500; product code ab150061; both from Abcam) secondary antibodies at room temperature for 1 h. After washing, DNA was counter-stained with DAPI (Sigma-Aldrich; Merck KGaA) at room temperature for 15 min, and images of 3 high-expression fields were captured using a fluorescence microscope (magnification, x200).

Western blot analysis. Antibodies raised against matrix metalloproteinase (MMP)-2, MMP-9, E-cadherin, N-cadherin, vimentin, Snail, PI3K, phosphorylated (p)-PI3K, AKT and p-AKT and CSC markers (ALDH1, CD133, Oct4 and Sox2) were used in the present study. GAPDH was selected as a reference protein. The information regarding the antibodies is summarized in Table I. The antibody of ALDH1 with cat. no. 22109-1-AP was used in 786-O cells, and the antibody of ALDH1 with product code ab52492 was used in ACHN cells. The antibody of GAPDH, cat. no. 10494-1-AP was used in 786-O cells, and antibody cat. no. 60004-1-Ig was used in ACHN cells. The 786-O and ACHN cells were cultured under normal conditions, and were then treated with parthenolide at various concentrations (0, 4 and 8 μM) for 24 h. The cells were scraped on the ice, collected by centrifugation (12,000 x g, 10 min, 4˚C) for protein extraction and incubated with freshly prepared RIPA lysis (Merck KGaA) for 15 min, and then quantified with a bicinchoninic acid (BCA) kit (Nanjing KeyGen Biotech. Co., Ltd.). The protein sample (20 μg) was mixed with loading buffer and boiled for 8 min. Subsequently, the sample was separated by a 10% SDS-PAGE gel and electrotransfered onto PVDF membranes (Merck KGaA). The membranes were incubated for 1 h at room temperature with 5% fat-free milk in Tris-buffered saline containing 10% Tween-20, followed by incubation overnight at 4˚C with primary antibodies. The following day, the cells were washed and incubated with secondary antibodies, AffiniPure goat anti-rabbit IgG (cat. no. 111-035-003) or anti-mouse IgG (cat. no. 115-035-003; both 1:3,000; both from Jackson ImmunoResearch, Inc.), at room temperature for 1 h. After washing, the protein bands were detected using an enhanced chemiluminescence (ECL) kit (Advansta, Inc.) and were analyzed by ImageJ software (v1.47; Rawak Software, Inc.).

Statistical analysis. GraphPad Prism 5.0 software (GraphPad Software, Inc.) was used for all statistical analyses. Results are presented as the mean ± standard deviation (SD) or standard error of the mean. Statistical significance was determined using ANOVA analysis followed by Tukey's post hoc test. $P<0.05$ was considered to indicate a statistically significant difference.

Results

Parthenolide suppresses the growth of human renal cancer cells. Parthenolide (Fig. 1A) was revealed to exert an effect on the viability of human 786-O and ACHN cells, which was examined by CCK-8 assay. It was revealed that the groups treated with various concentrations of parthenolide exhibited reduced cell survival rates (Fig. 1B and C).

To further confirm the effects of parthenolide on RCC, colony-formation assays were performed. Parthenolide significantly inhibited the colony-formation abilities of the 786-O and ACHN cells in a dose-dependent manner (Fig. 1D and E). These results indicated that parthenolide exerted an evident inhibitory effect on human RCC.

Parthenolide inhibits the migration and invasion abilities of RCC cells. To elucidate the underlying mechanisms of the effects of parthenolide on cell migration and invasion, the expression of related proteins was examined in the 786-O and

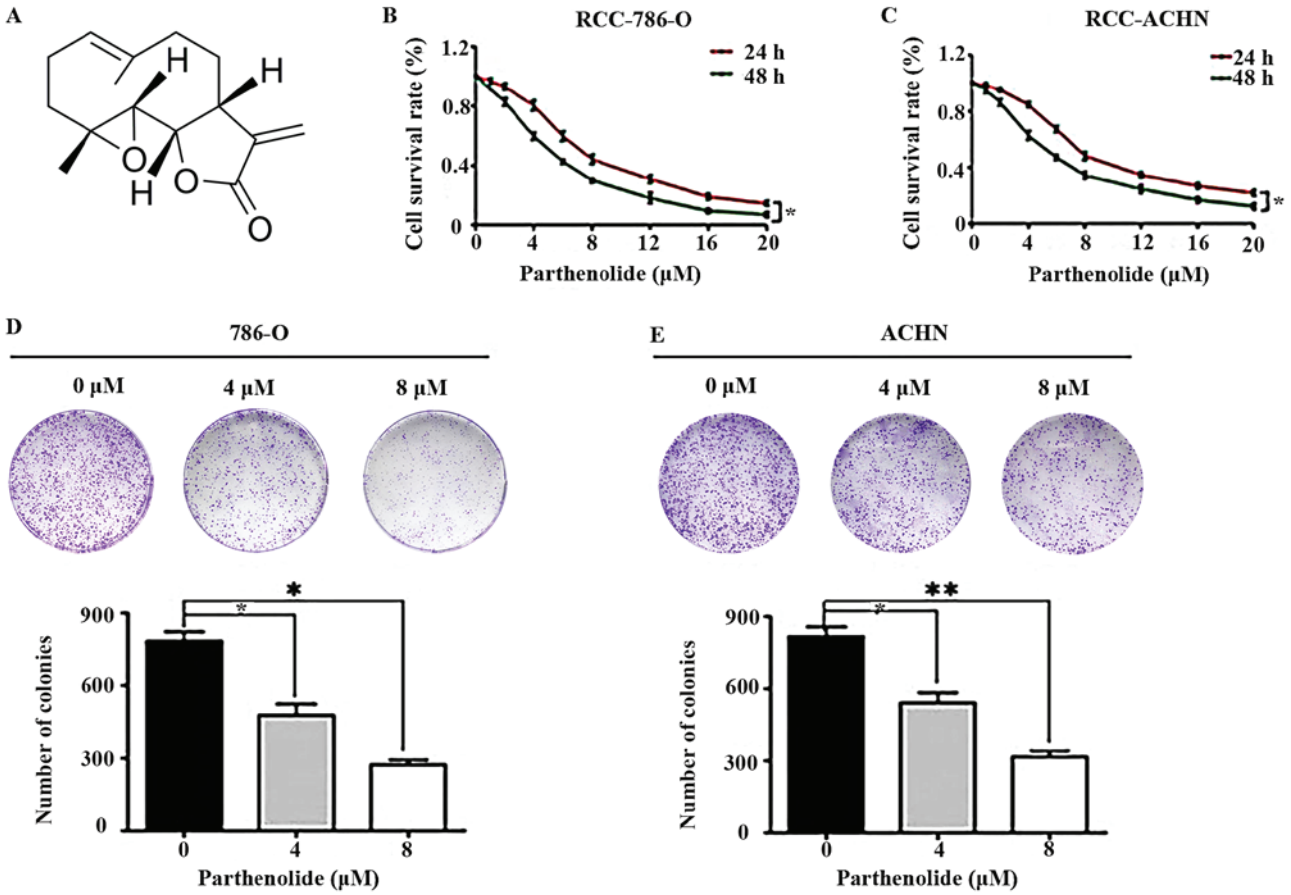

Figure 1. Effects of parthenolide on RCC. (A) Chemical structure of parthenolide. (B and C) 786-O and ACHN cells were treated with parthenolide (0, 1, 2, 4, 6, 8, 12, 16, 20 μM) for 24 and 48 h. Parthenolide suppressed the growth of these two cell lines in a dose-dependent manner. (D and E) Colony-formation assays demonstrated the inhibitory effects of parthenolide on 786-O and ACHN. Cells were grown in 6-well plates for 7 days following parthenolide (0, 4 and 8 μM) treatment. Parthenolide inhibited the colony formation of the two RCC cell lines in a dose-dependent manner. These experiments were performed 3 times. *P<0.05 and **P<0.01. RCC, renal cell carcinoma.

ACHN cells by western blot analysis. The results revealed that parthenolide decreased the expression of MMP-2 and MMP-9 in the 786-O and ACHN cells (Fig. 2).

Transwell assays demonstrated that the parthenolide-treated 786-O and ACHN cells exhibited suppressed migratory and invasive abilities compared with the control group (Fig. 3).

Effect of parthenolide on EMT of RCC cells. E-cadherin, N-cadherin and vimentin are important biomarkers of EMT. Western blot analysis was thus performed to examine the occurrence of EMT. The results revealed a high expression level of E-cadherin, and a low expression level of N-cadherin and vimentin in the 786-O and ACHN cells treated with parthenolide in a dose-dependent manner (Fig. 4A and B). The expression of E-cadherin and Snail was also assessed by RT-qPCR. The results revealed the increased expression of E-cadherin and the decreased expression of Snail (Fig. 4C and D) in the cells treated with parthenolide. Furthermore, the present study confirmed that parthenolide treatment induced high expression levels of E-cadherin, and decreased expression levels of N-cadherin and vimentin, as revealed by immunofluorescence (Fig. 5).

Additionally, the expression of the EMT transcriptional factor, Snail, was assessed by western blot analysis, which revealed that parthenolide treatment of the 786-O and ACHN cells inhibited the expression of Snail (Fig. 4A and B). The inhibited expression of Snail was also observed in the 786-O and ACHN cells treated with parthenolide by immunofluorescence (Fig. 5).

Parthenolide suppresses RCC cells stemness. Mammosphere formation is a typical cancer stem-cell property, which can reflect the self-renewal potential ability (15). Mammosphere formation assays were performed and they revealed that parthenolide significantly inhibited the number of spheres that derived from 786-O and ACHN cells (Fig. 6A). Western blot assays were also carried out to confirm whether parthenolide has an effect on cancer stem cell markers. The results revealed that parthenolide inhibited the expression of ALDH1, CD133, Oct4 and Sox2 (Fig. 6B).

Parthenolide suppresses the PI3K/AKT pathway. The PI3K/AKT pathway is one of the most frequently mutated or altered pathways in RCC and plays an important role in tumorigenesis, proliferation, and cancer progression. PI3K and AKT, which are the major components of this signaling pathway, are both increased in RCC (16). Parthenolide decreased the levels of components of the PI3K/AKT pathway including the expression of p-PI3K, and p-AKT (Fig. 7A and B). The total protein levels of PI3K, and AKT were also inhibited

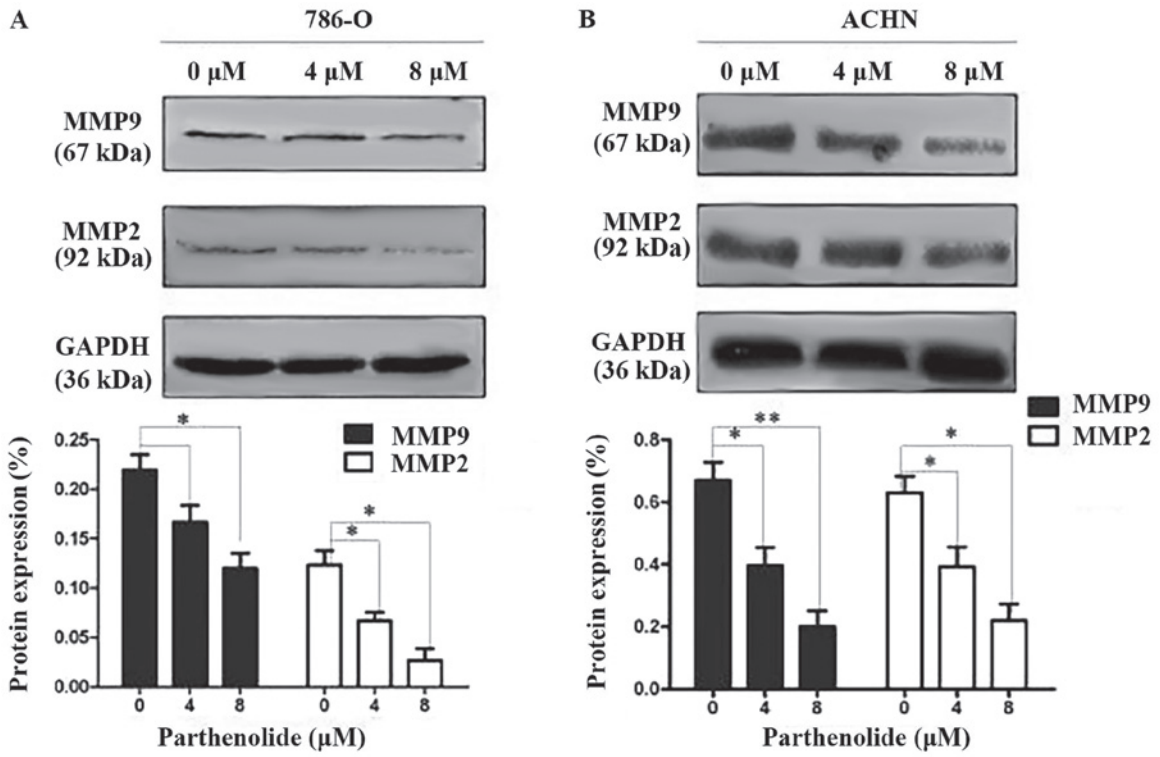

Figure 2. Parthenolide inhibits the migration of RCC cells. (A and B) RCC cells were treated with parthenolide (0, 4 and 8 μM) for 24 h. Parthenolide treatment led to a dose-dependent decrease in the expression levels of MMP-2 and MMP-9. *P<0.05, **P<0.01 vs. the control group. RCC, renal cell carcinoma.

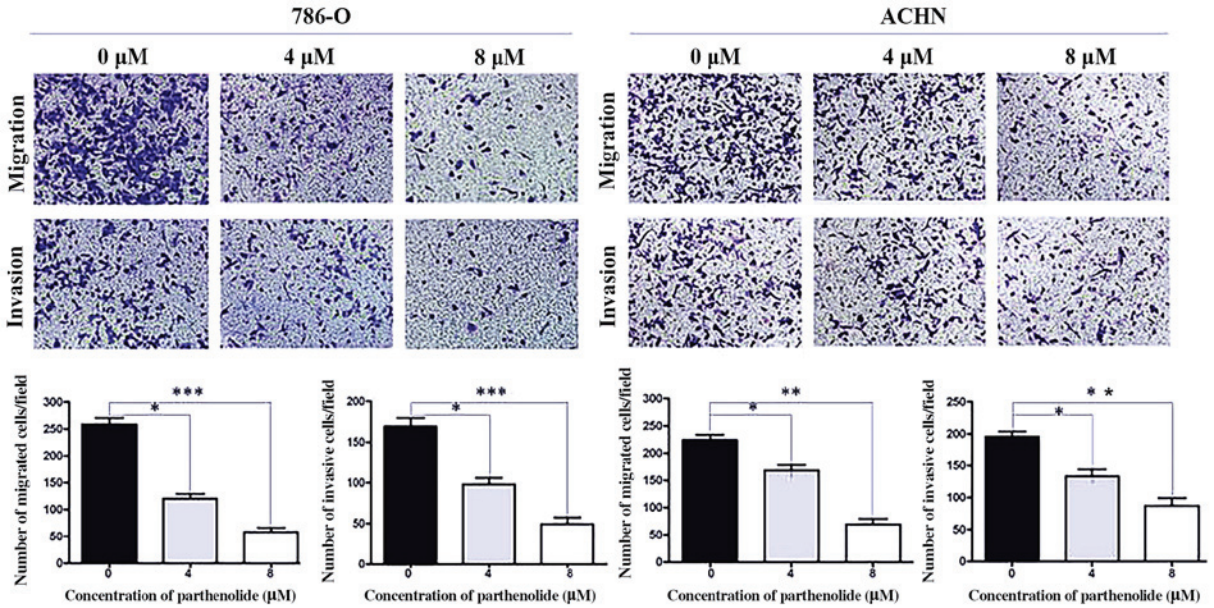

Figure 3. Parthenolide inhibits the migration and invasion abilities of RCC cells. Cells were treated with parthenolide at various concentrations (0, 4 and 8 μM) for 24 h. Representative images are presented, demonstrating that parthenolide inhibited the migration and invasion abilities of 786-O and ACHN cells. The number of cells in each field was counted, averaged and data are expressed as the means ± SD from 3 independent experiments. *P<0.05, **P<0.01 and ***P<0.001 vs. the control group. RCC, renal cell carcinoma.

by parthenolide, as determined by western blot analysis in 786-O and ACHN cells (Fig. 7A and B). The ratio of p-PI3K/PI3K and p-AKT/ AKT in 786-O and ACHN cells was also analyzed (Fig. 7C). There was no significant difference in the ratio of p-PI3K/PI3K between the control group and the group treated with 4 μM parthenolide in 786-O cells. The ratio of p-PI3K/PI3K was significant between the control group and the group treated with 8 μM parthenolide in 786-O cells. Similarly, no significant difference was observed in the ratio of p-AKT/AKT between the control group and the group treated with 4 μM parthenolide in 786-O cells. A significant difference was detected in the ratio of p-AKT/AKT between

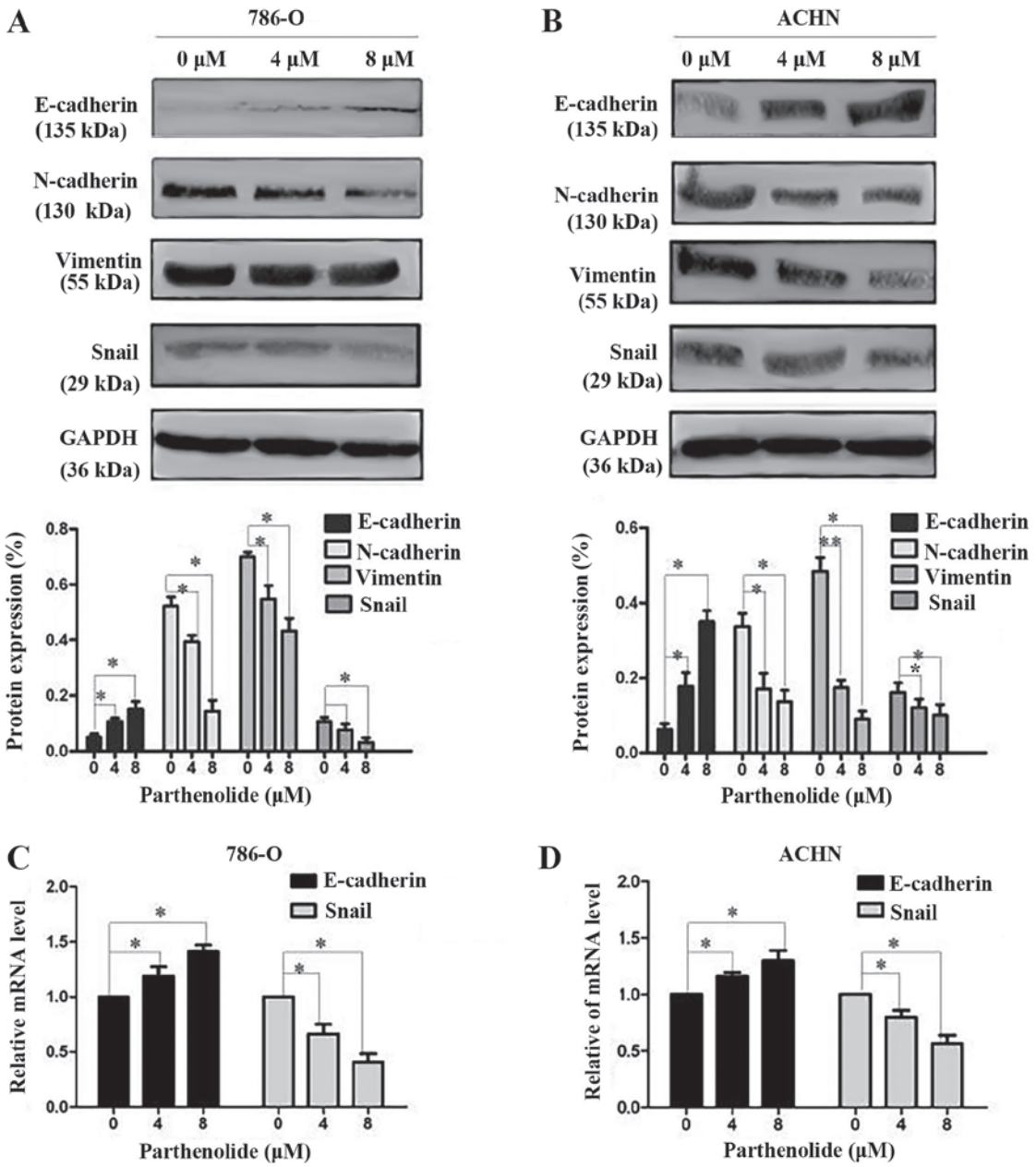

Figure 4. Parthenolide inhibits EMT biomarker expression in RCC cells. (A and B) Parthenolide (0, 4 and 8 μM) treatment increased the expression of E-cadherin and decreased N-cadherin and vimentin expression in a dose-dependent manner, as revealed by western blot analysis. Parthenolide treatment resulted in a decrease in the expression of Snail, as revealed by western blot analysis. (C and D) Parthenolide treatment increased the expression of E-cadherin and decreased the expression of Snail as determined by RT-qPCR. *P<0.05 and **P<0.01 vs. the control group. ETM, epithelial-mesenchymal transition; RCC, renal cell carcinoma; RT-qPCR, reverse transcription-quantitative polymerase chain reaction.

the control group and the group treated with 8 μM parthenolide in 786-O cells. In addition, there was no significant difference observed in the ratio of p-PI3K/PI3K between the control group and the groups treated with 4 and 8 μM with parthenolide in ACHN cells. However, a significant difference was observed in the ratio of p-AKT/AKT between the control group and the group treated with 8 μM parthenolide in ACHN cells.

Discussion

Renal cell carcinoma (RCC) comprises approximately 4.2% of all new cancer diagnoses, and RCC accounts for approximately 2-3% of adult malignant tumors and 80-90% of adult kidney malignancies (17). Therefore, it is of utmost importance to identify novel treatment strategies for RCC.

The sesquiterpene parthenolide has traditionally been used primarily for the treatment of fever, migraine and arthritis (6,18) and no significant side-effects have been reported in humans (19). In recent years, it has been revealed that parthenolide exerts anticancer effects against various types of tumors, such as breast cancer, cholangiocarcinoma, pancreatic, bladder and prostate cancer, as well as leukemia, and melanoma (20), which may be related to feverfew lactone; its structural formula contains a-methylene-γ-lactone ring and epoxide structure (21). As these structures can interact with

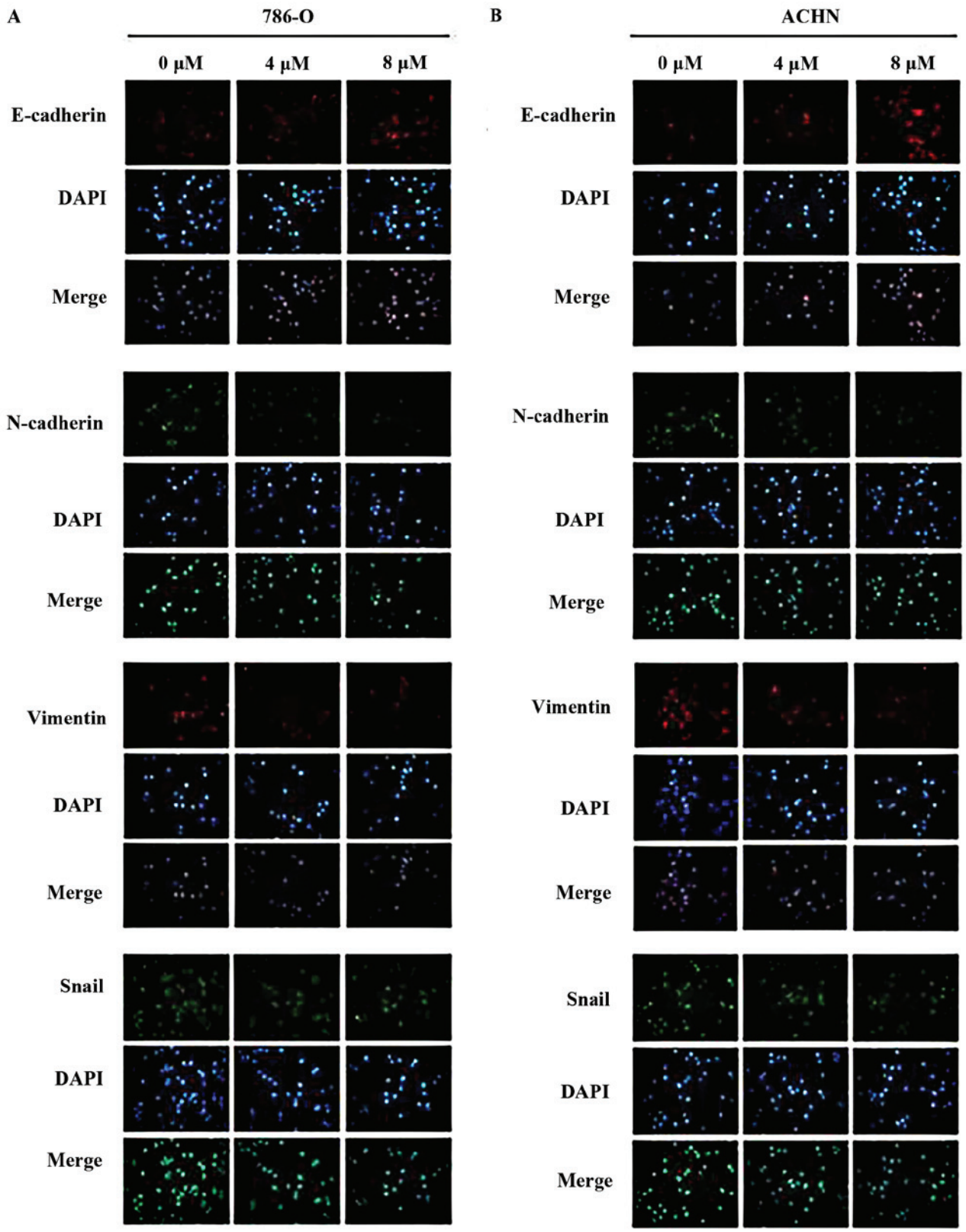

Figure 5. Expression of genes of EMT in 786-O and ACHN cell lines. (A and B) Cells were treated with parthenolide (0, 4 and 8 μM) for 24 h. Cells were processed and mounted on slides, and images were captured using a fluorescence microscope (magnification, x200). Red fluorescence indicates the presence of E-cadherin and vimentin; green fluorescence indicates N-cadherin and Snail; blue represents DAPI. Parthenolide treatment upregulated the expression of E-cadherin and decreased the expression of vimentin, N-cadherin and Snail. ETM, epithelial-mesenchymal transition.

enzymes and some functional proteins containing sulfhydryl groups, they can subsequently affect biological processes, such as cell signaling pathways, cell proliferation and apoptosis (22).

The present study revealed that parthenilide markedly inhibited the tumorous characteristics of 786-O and ACHN cells (Fig. 8). The results of CCK-8 assays indicated a marked

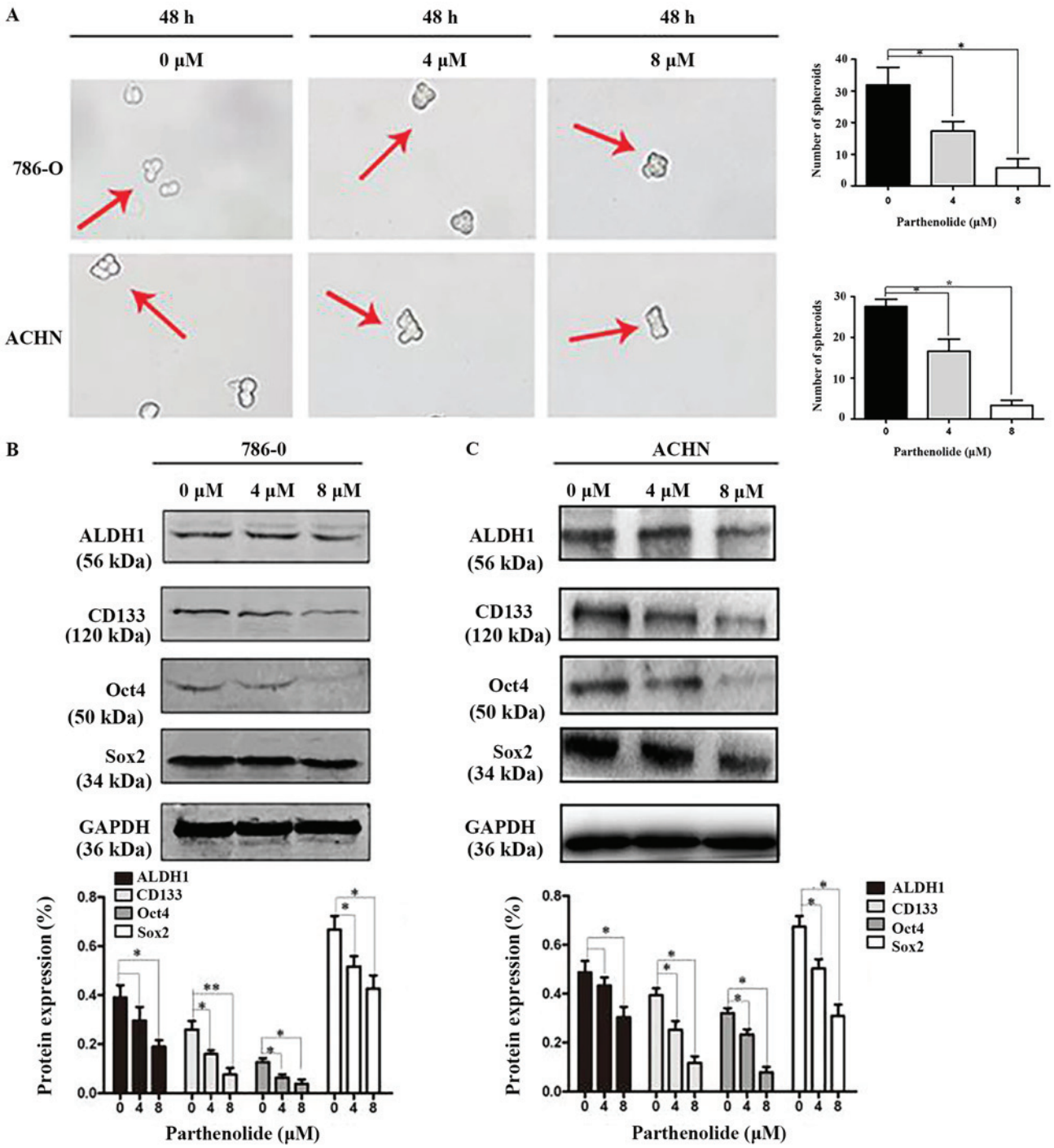

Figure 6. Parthenolid suppresses stem cell-like properties of RCC cells. (A) Mammosphere formation assay was performed to elucidate the inhibitory effects of Parthenolide on mammosphere formation. Mammosphere formation was inhibited in a dose-dependent manner in the 786-O and ACHN cell lines. (B and C) The expression of cancer stem cell markers was observed by western blot analysis. 786-O and ACHN cell lines treated with parthenolide (0, 4 and 8 μM) exhibited a lower expression of ALDH1, CD133, Oct4 and Sox2. *P<0.05 and **P<0.01 vs. the control group. RCC, renal cell carcinoma.

decrease in the viability of cancer cells following treatment with parthenolide, which occurred in a dose-dependent manner. Additionally, a colony-formation assay revealed that parthenolide suppressed the growth of the cells. Transwell assays revealed that parthenolide suppressed the migratory and invasive abilities of the 786-O and ACHN cells. Collectively, these data indicated that treatment with parthenolide may be a novel therapeutic strategy for RCC. In the present study, it was demonstrated that parthenolide suppressed the formation of mammospheres, which indicated parthenolide can inhibit renal cancer stem cell-like properties. In addition, the results of western blot analysis revealed that parthenolide exerted a significant effect on biomarkers of metastasis and EMT.

Invasion and metastasis are important biological features of malignant tumors. These biological processes can cause cancer cells to invade and spread to other tissues and organs, and represent a major obstacle to treatment (23). MMPs are zinc-dependent endopeptidases that play an important role in tumorigenesis and cancer cell development (24). They can degrade the main components of the basal membrane and

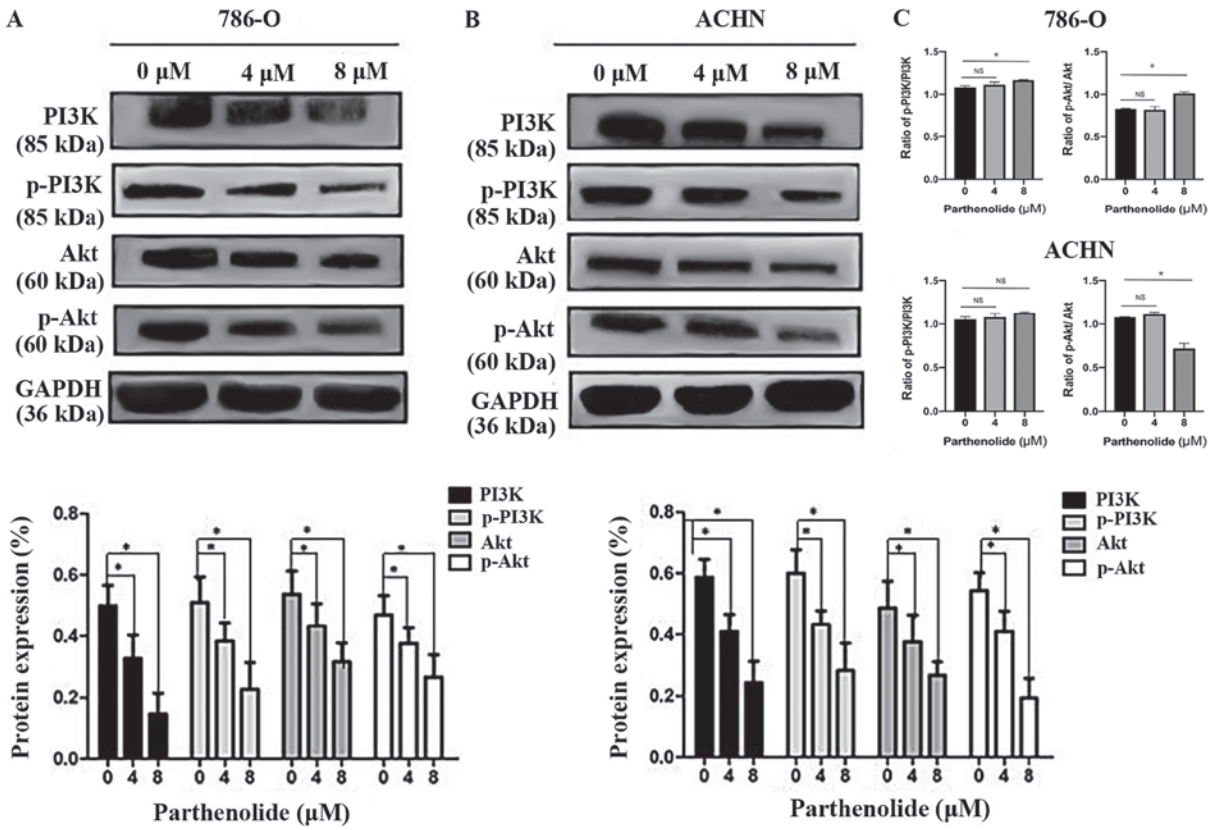

Figure 7. Parthenolide inhibits the PI3K/AKT pathway. (A and B) The expression of PI3K, p-PI3K, AKT and p-AKT was reduced in 786-O and ACHN cell lines with parthenolide treatment compared with control group. (C) The ratio of p-PI3K/ PI3K and p-AKT/AKT was increased in 786-O cells with treated with parthenolide compared with the control group. The ratio of p-PI3K/ PI3K was increased in ACHN cells treated with 4 and 8 μM parthenolide compared with the control group, however the differences were not significant. The ratio of p-AKT/AKT was increased in ACHN with 4 μM parthenolide compared with the control group, however the difference was not significant. The ratio of p-AKT/AKT was significantly decreased in ACHN cells treated with 8 μM parthenolide compared with the control group. *P<0.05. p-, phosphorylated.

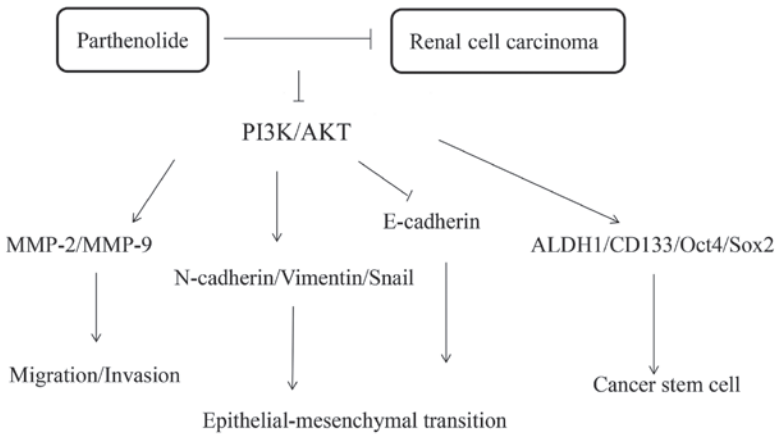

Figure 8. Parthenolide inhibits the tumorous characteristics of renal cell carcinoma.

extracellular matrix, such as collagen IV and fibronectin (25), causing a partial defect to the basement membrane, which promotes the passage of cancer cells, migration into blood vessels and lymphatic vessels, or other parts of the body cavity, followed by extended growth. It has been demonstrated that the overexpression of MMP-2 and MMP-9 is associated with a poor prognosis of RCC (26).

EMT refers to the loss of polarity of cells exhibiting an epithelial-like phenotype, demonstrating an enhanced mobility, the ability to move freely within the cell matrix and the transformation process of a fibroid phenotype (27). It has been demonstrated that EMT is closely related to the primary and secondary metastases of multiple tumor cells (28). The most significant change associated with EMT is the decrease in E-cadherin expression as an epithelial marker and the increase in N-cadherin expression as a mesenchymal marker (29). It is usually accompanied by the increased expression of stromal cell-derived proteins, such as vimentin, α-smooth muscle actin

and fibronectin (30). EMT activation is regulated by transcription factors, such as Snail. It has been revealed that Snail is a binding protein containing a zinc finger structure (31). It can recognize and combine with the F-box sequence of the E-cadherin gene promoter to inhibit the expression of E-cadherin and lead to the occurrence of EMT (32). The highly conserved Twist can promote the expression of Snail and further promote the tumor cells to undergo EMT (33).

The PI3K/AKT pathway is closely associated with tumorigenesis, growth, apoptosis, invasion, metastasis, EMT and the stem-like phenotype of cancer cells (34). The present results revealed that parthenolide could inhibit the PI3K/AKT pathway, which may be a potential mechanism of suppressing cancer cells. We only carried out the study *in vitro*, it is important and necessary to observe the function of parthenolide *in vivo*. In additional, the mechanism of parthenolide should be further studied in RCC.

In conclusion, the antitumor effects of parthenolide on RCC were demonstrated. The biological function of parthenoliode on renal cancer cells may be related to the regulation of the PI3K/AKT pathway. These findings provide a promising treatment approach for RCC.

Acknowledgements

We are grateful to the members of the Department of Pathology of Dalian Medical University (Dalian, China) for their discussion and suggestions during the course of this study.

Funding

No funding was received.

Availability of data and materials

The datasets used during the present study are available from the corresponding author upon reasonable request.

Authors' contributions

DL and YH contributed to the design and writing of the study. LeL and XR acquired and analyzed the data. DL, YH, HZ performed the experiments. SF and TQ made substantial contributions to the interpretation and analysis of the data. YH and LiL contributed to drafting the manuscript, revising it critically for important intellectual content. All authors read and approved the final manuscript.

Ethics approval and consent to participate

Not applicable.

Patient consent for publication

Not applicable.

Competing interests

The authors declare that they have no competing interests.

References

1. Erickson LA: Clear cell renal cell carcinoma. Mayo Clin Proc 93: 813-814, 2018.
2. Liu L, Wang Q, Mao J, Qin T, Sun Y, Yang J, Han Y, Li L and Li Q: Salinomycin suppresses cancer cell stemness and attenuates TGF-β-induced epithelial-mesenchymal transition of renal cell carcinoma cells. Chem Biol Interact 296: 145-153, 2018.
3. Siegel RL, Miller KD and Jemal A: Cancer statistics, 2015. CA Cancer J Clin 65: 5-29, 2015.
4. Escudier B, Pluzanska A, Koralewski P, Ravaud A, Bracarda S, Szczylik C, Chevreau C, Filipek M, Melichar B, Bajetta E, *et al*: Bevacizumab plus interferon alfa-2a for treatment of metastatic renal cell carcinoma: A randomised, double-blind phase III trial. Lancet 370: 2103-2111, 2007.
5. Singer EA, Gupta GN and Srinivasan R: Update on targeted therapies for clear cell renal cell carcinoma. Curr Opin Oncol 23: 283-289, 2011.
6. Bork PM, Schmitz ML, Kuhnt M, Escher C and Heinrich M: Sesquiterpene lactone containing Mexican Indian medicinal plants and pure sesquiterpene lactones as potent inhibitors of transcription factor NF-kappaB. FEBS Lett 402: 85-90, 1997.
7. Yang C, Yang QO, Kong QJ, Yuan W and Ou Yang YP: Parthenolide induces reactive oxygen species-mediated autophagic cell death in human osteosarcoma cells. Cell Physiol Biochem 40: 146-154, 2016.
8. Liu W, Wang X, Sun J, Yang Y, Li W and Song J: Parthenolide suppresses pancreatic cell growth by autophagy-mediated apoptosis. Onco Targets Ther 10: 453-461, 2017.
9. Marino S, Bishop RT, Carrasco G, Logan JG, Li B and Idris AI: Pharmacological inhibition of NFκB reduces prostate cancer related osteoclastogenesis in vitro and osteolysis ex vivo. Calcif Tissue Int 105: 193-204, 2019.
10. Diepenbruck M and Christofori G: Epithelial-mesenchymal transition (EMT) and metastasis: Yes, no, maybe? Curr Opin Cell Biol 43: 7-13, 2016.
11. Bai Y, Sha J and Kanno T: The role of carcinogenesis-related biomarkers in the Wnt pathway and their effects on epithelial-mesenchymal transition (EMT) in oral squamous cell carcinoma. Cancers (Basel) 12: 555, 2020.
12. Han X, Piao L, Yuan X, Wang L, Liu Z and He X: Knockdown of NSD2 suppresses renal cell carcinoma metastasis by inhibiting epithelial-mesenchymal transition. Int J Med Sci 16: 1404-1411, 2019.
13. Corrò C, Healy ME, Engler S, Bodenmiller B, Li Z, Schraml P, Weber A, Frew IJ, Rechsteiner M and Moch H: IL-8 and CXCR1 expression is associated with cancer stem cell-like properties of clear cell renal cancer. J Pathol 248: 377-389, 2019.
14. Livak KJ and Schmittgen TD: Analysis of relative gene expression data using real-time quantitative PCR and the 2(-Delta Delta C(T)) method. Methods 25: 402-408, 2001.
15. Xu C, Sun X, Qin S, Wang H, Zheng Z, Xu S, Luo G, Liu P, Liu J, Du N, *et al*: Let-7a regulates mammosphere formation capacity through Ras/NF-κB and Ras/MAPK/ERK pathway in breast cancer stem cells. Cell Cycle 14: 1686-1697, 2015.
16. Gargalionis AN, Sarlani E, Stofas A, Malakou LS, Adamopoulos C, Bamias A, Boutati E, Constantinides CA, Stravodimos KG, Piperi C, *et al*: Polycystin-1 induces activation of the PI3K/AKT/mTOR pathway and promotes angiogenesis in renal cell carcinoma. Cancer Lett 489: 135-143, 2020.
17. Siegel RL, Miller KD and Jemal A: Cancer statistics, 2018. CA Cancer J Clin 68: 7-30, 2018.
18. Murphy JJ, Heptinstall S and Mitchell JR: Randomised double-blind placebo-controlled trial of feverfew in migraine prevention. Lancet 2: 189-192, 1988.
19. Ghorbani-Abdi-Saedabad A, Hanafi-Bojd MY, Parsamanesh N, Tayarani-Najaran Z, Mollaei H and Hoshyar R: Anticancer and apoptotic activities of parthenolide in combination with epirubicin in mda-mb-468 breast cancer cells. Mol Biol Rep 47: 5807-5815, 2020.
20. Berdan CA, Ho R, Lehtola HS, To M, Hu X, Huffman TR, Petri Y, Altobelli CR, Demeulenaere SG, Olzmann JA, *et al*: Parthenolide covalently targets and inhibits focal adhesion kinase in breast cancer cells. Cell Chem Biol 26: 1027-1035,e22, 2019.
21. Dandawate PR, Subramaniam D, Jensen RA and Anant S: Targeting cancer stem cells and signaling pathways by phytochemicals: Novel approach for breast cancer therapy. Semin Cancer Biol 40-41: 192-208, 2016.

22. Freund RRA, Gobrecht P, Moser P, Fischer D and Arndt HD: Synthesis and biological profiling of parthenolide ether analogs. Org Biomol Chem 17: 9703-9707, 2019.
23. Liao L, Zhang L, Yang M, Wang X, Huang W, Wu X, Pan H, Yuan L, Huang W, Wu Y and Guan J: Expression profile of SYNE3 and bioinformatic analysis of its prognostic value and functions in tumors. J Transl Med 18: 355, 2020.
24. Li X, Kong L, Yang Q, Duan A, Ju X, Cai B, Chen L, An T and Li Y: Parthenolide inhibits ubiquitin-specific peptidase 7 (USP7), Wnt signaling, and colorectal cancer cell growth. J Biol Chem 295: 3576-3589, 2020.
25. Gonzalez-Avila G, Sommer B, García-Hernández AA and Ramos C: Matrix metalloproteinases' role in tumor microenvironment. Adv Exp Med Biol 1245: 97-131, 2020.
26. Bates AL, Pickup MW, Hallett MA, Dozier EA, Thomas S and Fingleton B: Stromal matrix metalloproteinase 2 regulates collagen expression and promotes the outgrowth of experimental metastases. J Pathol 235: 773-783, 2015.
27. Tiwari N, Gheldof A, Tatari M and Christofori G: EMT as the ultimate survival mechanism of cancer cells. Semin Cancer Biol 22: 194-207, 2012.
28. Luo F, Zhao Y and Liu J: Cell adhesion molecule 4 suppresses cell growth and metastasis by inhibiting the Akt signaling pathway in non-small cell lung cancer. Int J Biochem Cell Biol 123: 105750, 2020.
29. Sakamoto K, Imanishi Y, Tomita T, Shimoda M, Kameyama K, Shibata K, Sakai N, Ozawa H, Shigetomi S, Fujii R, *et al*: Overexpression of SIP1 and downregulation of E-cadherin predict delayed neck metastasis in stage I/II oral tongue squamous cell carcinoma after partial glossectomy. Ann Surg Oncol 19: 612-619, 2012.
30. Xi W, Sonam S, Beng Saw T, Ladoux B and Teck Lim C: Emergent patterns of collective cell migration under tubular confinement. Nat Commun 8: 1517, 2017.
31. Dattoli AA, Hink MA, DuBuc TQ, Teunisse BJ, Goedhart J, Röttinger E and Postma M: Domain analysis of the Nematostella vectensis SNAIL ortholog reveals unique nucleolar localization that depends on the zinc-finger domains. Sci Rep 5: 12147, 2015.
32. Georgakopoulos-Soares I, Chartoumpekis DV, Kyriazopoulou V and Zaravinos A: EMT factors and metabolic pathways in cancer. Front Oncol 10: 499, 2020.
33. Škovierová H, Okajčeková T, Strnádel J, Vidomanová E and Halašová E: Molecular regulation of epithelial-to-mesenchymal transition in tumorigenesis (Review). Int J Mol Med 41: 1187-1200, 2018.
34. Jiang N, Dai Q, Su X, Fu J, Feng X and Peng J: Role of PI3K/AKT pathway in cancer: The framework of malignant behavior. Mol Biol Rep 47: 4587-4629, 2020.